Framework Zinc-Substituted Zeolites: Synthesis, and Core-Level and Valence-Band XPS

Robert A. Hunsicker and Kamil Klier*

Department of Chemistry and Zettlemoyer Center for Surface Studies, Lehigh University, Bethlehem, Pennsylvania 18015

Thomas S. Gaffney and John G. Kirner

Air Products and Chemicals, Inc., 7201 Hamilton Boulevard, Allentown, Pennsylvania 18195-1501

Received June 14, 2002. Revised Manuscript Received August 23, 2002

A proof of framework substitution of T atoms of faujasite by divalent zinc is obtained by high-resolution X-ray photoelectron spectroscopy (XPS). Distinct and systematic XPS binding energy shifts between cationic and framework zinc are reported for both the core-levels and the valence-band Zn3d emission. A strong preference of T-atom substitution with zinc for silicon rather than aluminum is observed. Synthesis of a zinc-containing faujasite gives rise to a clean embedding of zinc into the framework. A subsequent postsynthesis modification by aqueous solution of zinc oxide in sodium hydroxide further enhances the framework zinc concentration. In the present investigation, a total of 15% Si atoms substituted by zinc yielded over a 2-fold enhancement of the monovalent cation-exchange capacity of faujasite.

Introduction

The substitution of divalent elements Me(II) for silicon into tetrahedral framework positions of silicates and aluminosilicates gives rise to two negative framework formal charges per $Me(II)_{Td}$ atom, and is accompanied by a charge-balancing cation-exchange capacity of two positive charge-equivalents per each $Me(II)_{Td}$. These two cationic charges may be realized by two monovalent cations such as Na(I) or a divalent cation such as Ca(II). The location and coordination of these cations is of importance in the formation of complexes with molecules which, in the case of microporous silicates such as zeolites, have access to the open coordination sphere of these cations. Weak molecule−cation complexes afford the opportunity for separation of individual molecular species from mixtures through subtle differences of the complexation strengths and diffusion rates. Of particular interest is the separation of the components of air such as oxygen, nitrogen, argon, etc. In the pressure-swing process,[1] *nontransition-metal cations* such as Ca(II) bind the N_2 molecules more strongly than O_2 due to the interaction of the molecular quadrupole moment of N_2 with the cationic charge;[2] on the other hand, certain *transition-metal cations* such as Cr(II) form stronger reversible dioxygen complexes[3] due to specific interactions between the open d-shell of Cr(II) with the O_2 molecule.[4]

The above observations and principles hold true if the synthesis is successful to the point at which no side processes thwart the desired cation and framework-substitute distribution, and the material is stable in a long use. The diagnostics of the synthesized, dehydrated, and used materials is of paramount importance for determining the efficiency of both the material synthesis and its function in separation processes. We have chosen high-resolution X-ray photoelectron spectroscopy in the core and the valence-band regions, supported by quantum mechanical calculations, to provide methodology for analysis of zeolite materials with a variety of framework-substituted atoms, cations, and intrazeolitic molecular complexes. This is a novel approach, as evidence for framework substitution has so far relied for the most part on elemental analysis, X-ray diffraction in an averaging manner, and solid-state NMR of elements other than those replacing the T-atoms.

In the present work, we report on the synthesis of Zn-framework-substituted faujasite (FAU),[5] Zn(II) cation-exchanged FAU, and the core-level and valence-band XPS spectra of these materials.

Zinc substitution into frameworks of both dense and microporous silicates and aluminiosilicates via synthesis has previously been claimed, probably for the first time, in a 1982 patent.[6] In this patent, structures of LTA[5]

* To whom correspondence should be addressed. Phone: 610-758-3577. Fax: 610-974-6469. E-mail: kk04@lehigh.edu.

(1) Breck, D. W. *Zeolite Molecular Sieves: Structure, Chemistry and Use*; J. Wiley & Sons: New York, 1974; pp 709−711.

(2) The electrostatic quadrupoles of the N_2 and O_2 molecules are 5.54×10^{-8} and 3.86×10^{-8} cm, respectively, as determined from NH_3 3,3 line broadening, cf. Hirschfelder, J. O.; Curtiss, C. F.; Bird, R. B. *Molecular Theory of Gases and Liquids*; Wiley & Sons: New York, 1954; p 1028.

(3) Kellerman, R.; Hutta, P. J.; Klier, K. *J. Am. Chem. Soc.* **1974**, *96*, 5946−5947.

(4) Klier, K. Electronic Structure of Transition-Metal Ion Containing Zeolites. In *Catalysis by Unique Metal Ion Structures in Solid Matrixes*; Centi, G., Wichterlová, B., and Bell, A. T., Eds.; NATO Science Series, Vol. 13; Kluwer Academic: Boston, MA, 2001; pp 115−133.

(5) Meier, W. M.; Olson, D. H. *Atlas of Zeolite Structure Types*, 2nd ed.; Butterworth: London, 1987.

10.1021/cm0206690 CCC: $22.00
Published on Web 10/08/2002

topology were reported and FAU was alluded to. However, little characterization to confirm the extent of framework incorporation was presented. In a more conclusive piece of work, Camblor, Lobo, Koller, and Davis[7] reported on framework zinc silicates and their synthesis, excepting faujasite, with ^{29}Si MAS NMR allowing predictions of structural details of tectozincosilicates VPI-7 and VPI-9 by Camblor and Davis.[8] In the faujasite family, the only two reports to our knowledge are the European Patent Application by Araya and Wirral[9] and a colloquium paper by Kowalak, Stawinski, Stankiewicz, and Dziedzic.[10] Kowalak et al. reported the preparation of zinc-containing molecular sieves including zincoaluminosilicates with the FAU, SOD, and MFI structures[5] and zincosilicates with unknown structures, but provided no evidence for zinc incorporation into the framework other than changes in catalytic activity that could just as well have resulted from extra-framework zinc.

We have synthesized faujasites with varying amounts of zinc substituted in the framework and provide herein evidence for framework substitution as well as a tool for distinguishing between cationic and framework zinc using high-resolution XPS and assignments of chemical shifts supported by theory.

Experimental Section

Materials. Four faujasite zeolites have been prepared aiming at various contents of framework zinc (Zn_{fr}) substituting for the framework T atoms, and cationic zinc (Zn_{cat}) substituting for the Na cations. The purpose of these preparations and XPS analysis was to obtain (a) a proof of framework substitution and (b) enhancement of cation-exchange capacity of faujasite, possibly of aluminosilicate materials in general. The samples and their properties were (1) NaY; (2) $NaZn_{exch}Y$; (3) $NaZn_{synth}Y$; and (4) $NaZn_{post}Y$, prepared as follows. NaY (1) was zeolite Y with no zinc. $NaZn_{exch}Y$ (2) was zeolite NaY partially exchanged with zinc from aqueous $Zn(NO_3)_2$. $NaZn_{synth}Y$ (3) was zeolite Y synthesized for framework substitution of T atom by zinc following closely ref 9, example 1. Specifically, a solution of 1.1 g of ZnO in 7.8 g of water and 7.5 g of NaOH was further diluted with 50.7 g of H_2O, and 15.4 g of $NaAlO_2$ solution (20 wt % Al_2O_3, 20 wt % Na_2O) was added. This solution was poured into a polypropylene bottle containing 48.5 g of Ludox HS 40 silica (40 wt % SiO_2, 0.43 wt % Na_2O). The mixture formed a gel which was shaken vigorously and aged for 24 h at room temperature. Subsequently, the bottle was placed in an oven at 95 °C for 7 days. The crystalline product was filtered, decanted with distilled water, filtered again, and dried in an oven at 95 °C for 24 h. Finally, $NaZn_{post}Y$ (4) was zeolite $NaZn_{synth}Y$ in which additional zinc was introduced by a postsynthesis modification with zinc oxide solution in sodium hydroxide (ref 9, example 5). Specifically, 5 g of $NaZn_{synth}Y$ synthesized as above was suspended in 250 mL of a solution containing 0.2 M ZnO and 2 M NaOH. This suspension was stirred at 95 °C for 5 h, filtered, washed with 0.25 M NaOH to remove excess zincate, washed with distilled water, and dried.

Table 1. Elemental Analysis, Powder X-ray Diffraction (XRD), and NMR Data for Faujasites with Varying Concentrations of Zinc Used in This Study

	NaY	$NaZn_{exch}Y$	$NaZn_{synth}Y$	$NaZn_{post}Y$
wt. % Al_2O_3	15.45	15.09	14.77	16.39
wt. % SiO_2	50.15	45.97	42.28	35.04
wt. % ZnO	-	4.70	3.79	7.03
wt. % Na_2O	9.31	6.16	13.10	13.50
LOI[a]	25.64	26.69	25.75	26.86
material balance	100.55	98.61	99.70	98.82
XRD phase	FAU	FAU	FAU	FAU
XRD a_0, nm	2.4629	2.4716	2.4763	2.4836
NMR nominal Si/Al	2.63		1.85	1.64
NMR Si(5Me) %[b]			1.83	2.09
NMR Si(4Me) %[b]	0.5		7.1	13.4
NMR Si(3Me) %[b]	9.4		28.2	34.4
NMR Si(2Me) %[b]	38.8		39.2	35.4
NMR Si(1Me) %[b]	41.3		19.0	11.8
NMR Si(0Me) %[b]	7.8		3.6	2.9

[a] Loss on incineration. [b] The abbreviation Si(nMe) denotes a framework Si atom connected to n nearest neighbors other than Si, i.e., Me = Al + Zn.

The compositions, structural parameters and NMR data of these samples are listed in Table 1.

XPS Analysis. *Instrumentation.* The instrument used was the Scienta ESCA 300 high-resolution X-ray photoelectron spectrometer located in the Zettlemoyer Center for Surface Studies at Lehigh University. The Scienta ESCA 300 utilizes a rotating Al Kα anode to generate an unpolarized 7.6 kW X-ray flux ($h\nu$ = 1486.8 eV), which was monochromatized by seven toroidally bent quartz crystals. The detector system, consisting of a 300-mm mean radius hemispherical electron energy analyzer and a multichannel plate detector, provides an overall energy resolution of 0.27 eV, as determined at room temperature by the Fermi level edge from Ag. The high sensitivity and energy resolution of the detector, combined with a charge-compensating hot filament electron flood gun with an energy range of 0−10 eV, allows for the analysis of insulated samples.

Sample Preparation and Transfer. Synthesis of the faujasite samples by was followed by dehydration under vacuum (10^{-6} Torr, turbo pump) with ramping temperature up to 400 °C, ramp rate 1 °C/minute, then held at 400 °C for the total time of 16 h. The dehydrated faujasite samples were attached with double-sided adhesive tape onto an ESCA analysis stub in a nitrogen-filled glovebox and flattened down with a spatula. The prepared stub was transferred in a desiccator from the glovebox to a nitrogen-filled glovebag attached to the fast-entry chamber of the Scienta spectrometer. After filling the glovebag to positive pressure with dry nitrogen and bringing the fast-entry chamber to atmospheric pressure, also with nitrogen, the prepared stub was transferred into the fast-entry chamber. The fast-entry chamber was then pumped down to pressures of 7.5×10^{-8} Torr.

Conditions for the Core-Level and Valence-Band XPS Analysis. Both survey and high-resolution scans were performed on each of the faujasite samples, with the pressure in the analysis chamber of 1.5×10^{-9} Torr. Survey scans were conducted with 300 eV pass energy, an incremental energy step size of 1 eV, and a 0.8-mm slit width. Scans of Na 1s, Zn 2p3/2, O 1s, C 1s, Si 2p, Al, 2p, Zn Auger, the sub-valance band, and the valence band were conducted at a high resolution mode with 150 eV pass energy, an incremental step size of 0.05 eV, and a 0.8-mm slit width. The pass energy refers to the energy to which the kinetic energy of the emitted photoelectrons was retarded by a retardation voltage for detection by the analyzer. The step size in turn refers to the energy step between each sweep of the retardation voltage. The slit width refers to the width of the slit located at the entrance to the detector. A larger slit width provides increased photoemission intensity with poorer resolution. Because the faujasites were nonconducting materials, a hot filament flood gun set at 2 eV was applied during the analysis to supply electrons for charge compensation and improve the quality of the resolution.

(6) McAnespie, P.; Dyer, A.; Mehta, B. J. U.S. Patent 4,329,328, 1982.
(7) Camblor, M. A.; Lobo, R. F.; Koller, H.; Davis, M. E. *Chem. Mater.* **1994**, *6*, 2193.
(8) Camblor, M. A.; Davis, M. E. *J. Phys. Chem.* **1994**, *98*, 13151.
(9) Araya, A.; Wirral, M. European Patent Application Pub. No 0 476 901 A2 (Sept. 9, 1991).
(10) Kowalak, S.; Stawinski, K.; Stankiewicz, K.; Dziedzic, A. Preparation and Properties of Zinc-Containing Molecular Sieves. In *Proceedings of the 3rd Polish-German Zeolite Colloquium*; Rozwadowski, M., Ed.; Nicholas Copernicus University Press: Torun, Poland, 1998; p 169.

Table 2. XPS Sensitivity Factors $S_{X,j}$ of *j*-th Photoemission from Element *X* for Analysis of Zinc Faujasites

photoelectron emission	BE/eV[a]	$S_{X,j}$
Al2p	75	0.705
Si2p	103	1.132
O1s	532	2.837
Zn2p$_{3/2}$	1023	18.920
Na1s	1073	8.520
C1s	285	1.000

[a] The binding energy BE = E(Al Kα) − E_k, where E(Al Kα) = 1486.6 eV and E_k is the kinetic energy of the photoelectron. Precise values of BEs are given in Table 3.

Sensitivity Factors for Quantitative XPS. Methods for quantitative XPS analysis of powdered materials, including those with nonuniform distribution of elements at the surface and in bulk, have been described previously.[11−13] Here, we simplify the analysis to describe average concentrations of elements within the escape depth of photoelectrons from a dry zeolite, estimated from the material's density at 3.4−4.7 nm. The analytical concentration c_X of an element X is calculated as $c_X = I_{X,j}/S_{X,j}(\lambda_j)$, where $I_{X,j}$ is the intensity of the j-th photoelectron line, $S_{X,j}(\lambda_j)$ is the sensitivity factor for that line, and λ_j is the escape depth in the given material for the j-th line. The λ_j depends on the kinetic energy E_k of the j-th photoemission, in our range approximately proportional to $E_k^{1/2}$.[14] The sensitivity factors applied here are a combination of the Scofield ionization cross sections,[15] the Scienta 300 response function, and calibrations using an NaCoA zeolite with the known Si/Al ratio 1:1. The values of $S_{X,j}$ are listed in Table 2.

Specific to the present investigation, the large $S_{Zn,2p}$ allows the detection and quantitative analysis of small concentrations of zinc. The saved files, identified as RHA065.001-0.008, can be read using Scienta ESCA software and are available from the authors.

Results

Core-Level and Valence-Band XPS. Significant uniform differences of photoelectron binding energies from the cationic and framework zinc species were observed herein. The results are summarized in Table 3 for the four faujasite materilas listed in the Experimental Section. Because of the required precision, the quality of charge neutralization is also documented by the narrow line widths.

The reference level to which all spectra were adjusted by a common shift of binding energies (BEs) to each, was chosen to be the Si2p emission. These shifts also brought to coincidence the top of the O2p valence band which validates the procedure given that Si and O are majority elements whose BEs are not expected to change upon substitutions by smaller amounts of zinc.

The Zn2p$_{3/2}$ lines of the NaZn$_{exch}$Y, NaZn$_{synth}$Y, and NaZn$_{post}$Y materials are shown in Figure 1. The NaZn$_{post}$Y preparation yielded a broader line centered between those for NaZn$_{exch}$Y and NaZn$_{synth}$Y, which could be resolved into two components with BEs of 1022.7 eV (fwhm 1.80 eV) and 1023.6 (fwhm 1.85 eV), yielding relative areas of 79.7% for the former and 20.3% for the latter component. The Zn3d lines that emerge within the O2p valence band show a pattern (Figure 2) similar to that of clearly separated Zn3d emissions in NaZn$_{exch}$Y and NaZn$_{synth}$Y, with NaZn$_{post}$Y broader and in between.

Table 3. Binding Energies (BE) and Linewidths (fwhm) in the Faujasites Studied

photoelectron emission	NaY	NaZn$_{exch}$Y	NaZn$_{synth}$Y	NaZn$_{post}$Y
		BE (eV)		
Na 1s	1073.19	1073.16	1073.40	1073.34
Zn 2p$_{1/2}$ [a]	- - - -	1046.3	1045.0	- - - -
Zn 2p$_{3/2}$	- - - -	1023.68	1022.62	1022.93
Zn 3s [a]	- - - -	141.8	140.6	141.2
Zn 3p$_{1/2}$ [a]	- - - -	94.2	93.1	93.0
Zn 3p$_{3/2}$ [a]	- - - -	90.8	89.6	90.2
O 1s	532.47	532.55	532.44	532.43
C 1s	284.91	285.04	285.41	285.67
Si 2p	103.38	103.38	103.38	103.38
Al 2p	74.81	74.99	75.11	75.32
Na 2p	32.17	32.32	32.39	32.29
O 2s	24.67	24.69	24.71	24.70
O 2p edges	15.01	15.25	15.02	14.50
	5.82	5.76	5.58	5.58
Zn 3d	- - - -	12.56	11.47	11.67
		fwhm (eV)		
Na 1s	1.76	1.77	1.80	2.00
Zn 2p$_{3/2}$	- - - -	1.85	1.80	1.84
O 1s	2.14	2.16	2.22	2.10
C 1s	1.26	1.53	1.43	1.55
Si 2p	1.67	1.73	1.70	1.80
Al 2p	1.40	1.60	1.37	1.55
Na 2p	1.56	1.59	1.63	1.81
O 2s	3.31	3.29	3.28	3.28
O 2p	9.19	9.49	9.44	8.92
Zn 3d	- - - -	1.85	1.41	1.68

[a] BE values taken from survey scan (step size 1.0 eV) with each peak fit by a Gaussian. The remaining BEs, accurate to within 10^{-2} eV, are from regional scans (step size 0.05 eV) around the given photoemissions specified in column 1. The fwhm (eV) values for the emissions from the regional scans are given in the second section of the table.

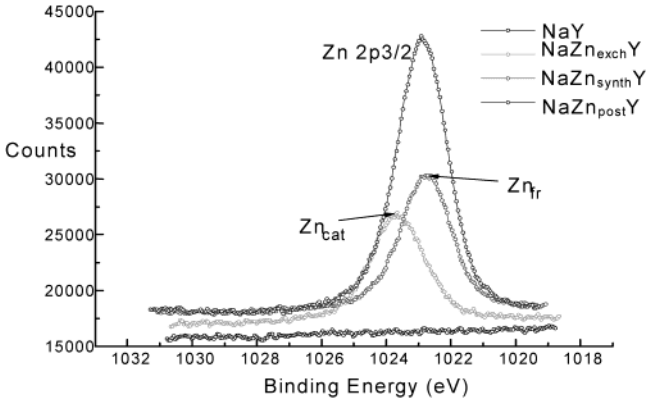

Figure 1. High-resolution photoelectron Al Kα spectra of the Zn 2p3/2 region of NaY, NaZn$_{exch}$Y, NaZn$_{synth}$Y, and NaZn$_{post}$Y faujasites taken at 150 eV pass energy. Zn$_{cat}$ is photoelectron emission from the cation-exchanged zinc in NaZn$_{exch}$Y, and Zn$_{fr}$ is from the framework-substituted zinc in NaZn$_{synth}$Y. The postsynthesis modified material, NaZn$_{post}$Y, shows a broader peak due to the presence of both Zn$_{cat}$ and Zn$_{fr}$.

Quantitative XPS. The XPS intensities of the Al2p, Si2p, Zn2p$_{3/2}$, Na1s, O1s, and C1s (impurity) lines were converted to concentrations c_{Al}−c_{Na} using sensitivity factors listed in Table 2 and further to atom percent values. The results are summarized in Table 4 and compared with bulk chemical analysis in terms of elemental ratios in Table 5.

(11) Vedage, G. A.; Himelfarb, P. B.; Simmons, G. W.; Klier, K. *ACS Symp. Ser.* **1985**, *279*, 295.
(12) Sojka, Z.; Klier, K. *J. Electron Spectrosc.* **1992**, *60*, 155.
(13) Simmons, G. W.; Angst, D. L.; Klier, K. *J. Electron Spectrosc. Relat. Phenom.* **1999**, *105*, 197.
(14) Chang, C. C. *Surface Sci.* **1975**, *48*, 9.
(15) Scofield, S. H. *J. Electron Spectrosc. Relat. Phenom.* **1976**, *8*, 129.

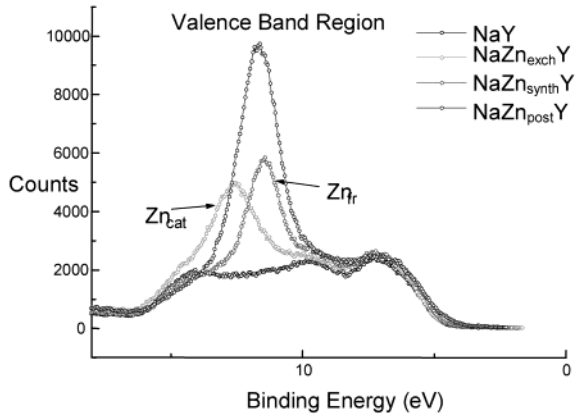

Figure 2. High-resolution photoelectron Al Kα spectra of the Valence Band region of NaY, NaZn$_{exch}$Y, NaZn$_{synth}$Y, and NaZn$_{post}$Y faujasites taken at 150 eV pass energy. Zn$_{cat}$ is photoelectron emission from the cation-exchanged zinc in NaZn$_{exch}$Y, and Zn$_{fr}$ is from the framework-substituted zinc in NaZn$_{synth}$Y. The postsynthesis modified material, NaZn$_{post}$Y, shows a broader peak due to the presence of both Zn$_{cat}$ and Zn$_{fr}$.

Table 4. HR-XPS Elemental Analysis (% Element) of the Faujasite Samples Studied

element	NaY	NaZn$_{exch}$Y	NaZn$_{synth}$Y	NaZn$_{post}$Y
Na 1s	7.139	4.592	9.377	10.605
Zn 2p3/2	- --	1.236	1.412	3.654
O 1s	56.177	54.167	54.814	51.626
C 1s	8.123	11.285	7.273	10.337
Si 2p	21.314	20.991	19.737	16.308
Al 2p	7.247	7.729	7.386	7.470

Table 5. Comparison of Chemical and XPS Elemental Analysis of the Faujasite Samples Studied

	NaY	NaZn$_{exch}$Y	NaZn$_{synth}$Y	NaZn$_{post}$Y
Chemical (Bulk) Analysis				
Si:Al	2.75:1	2.58:1	2.43:1	1.81:1
Si:(Al+Zn)	- - - -	- - - -	2.09:1	1.43:1
Si:Zn	- - - -	- - - -	15.10:1	6.75:1
Na:Si	- - - -	- - - -	0.60:1	0.75:1
Na:Al	0.99:1	0.67:1	1.46:1	1.36:1
Na:(Al + 2Zn)	- - - -	- - - -	1.10:1	0.88:1
Al:Zn	- - - -	- - - -	6.22:1	3.72:1
XPS Analysis				
Si2p:Al2p	2.941:1	2.716:1	2.672:1	2.183:1
Si2p:(Al2p +Zn2p3/2)	- - - -	- - - -	2.243:1	1.466:1
Si2p:Zn2p3/2	- - - -	- - - -	13.980:1	4.463:1
Na1s:Si2p	- - - -	- - - -	0.475:1	0.650:1
Na1s:Al2p	0.985:1	0.594:1	1.270:1	1.420:1
Na1s:(Al2p+ 2Znp3/2)	- - - -	- - - -	0.918:1	0.718:1
Al2p:Zn2p3/2	- - - -	- - - -	5.231:1	2.044:1
O1s:(Si2p + Al2p)	1.967:1	1.886:1	- - - -	- - - -

The chemical and XPS Si/Al ratios are to within relative 15% agreement for NaY, NaZn$_{exch}$Y, and NaZn$_{synth}$Y, with some evidence of zinc enrichment in the surface photoelectron escape region in the postsynthesis modified NaZn$_{post}$Y, where XPS shows a significantly (by 34%) lower Si/Zn ratio (4.463) than chemical analysis (6.75). The elemental ratios obtained by chemical and XPS analysis are graphically compared in Figure 3.

Discussion

The present results demonstrate the following points. (1) HR-XPS in both the core-level and the valence-band regions affords a reliable spectroscopic proof for framework substitution of a T atom by zinc and a clear-cut distinction between framework and cation-exchanged

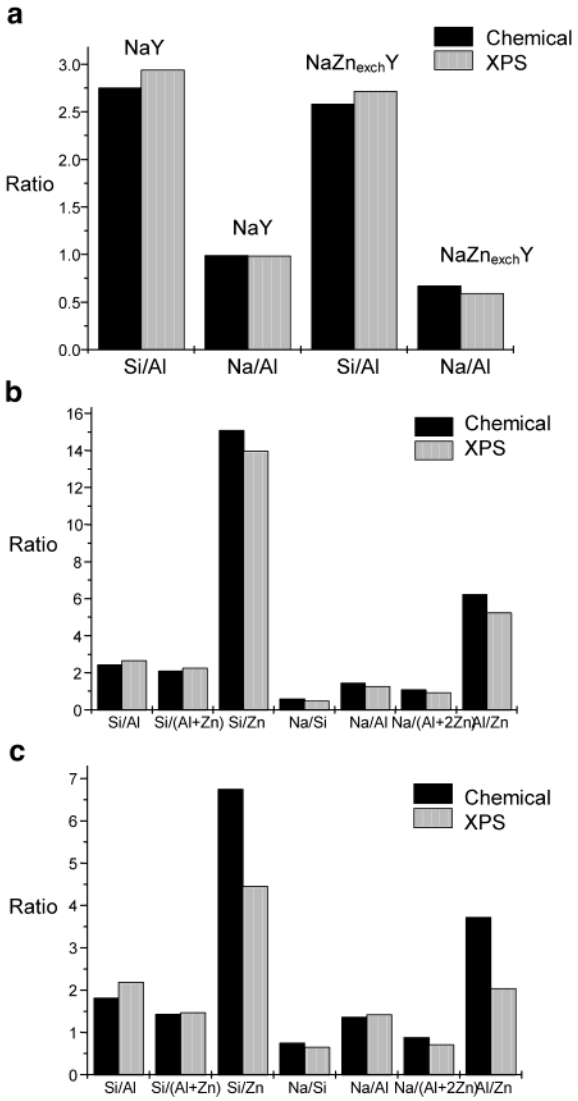

Figure 3. (a) Elemental analyses of NaY and NaZn$_{exch}$Y. (b) Elemental analyses of NaZn$_{synth}$Y. (c) Elemental analyses of NaZn$_{post}$Y.

zinc by BE shifts of Zn$_{cationic}$ from Zn$_{framework}$ by 1.3 eV (Zn2p$_{1/2}$) to 1.09 eV (Zn3d). (2) Synthesis of the framework-substituted Zn zeolite reported in the literature and herein is successful to place zinc exclusively as a substituent primarily for the Si framework atoms. (3) Postsynthesis modification with ZnO/NaOH enhances the concentration of framework zinc further by a factor of 2 to achieve 15 at. % T substitution, whereas a smaller amount (~4%) of zinc enters cation sites in this treatment.

The reason for the higher BE (i.e., more negative orbital energy) of Zn$_{cationic}$ from Zn$_{framework}$ can be envisioned, qualitatively, as originating from the more positive charge of Zn$_{cationic}$ compared to the formally "dinegative" framework zinc. Considerations of effective charges go beyond the simplistic ionic picture, however: the zinc bonding in both the cationic and the framework site is quite covalent, and the orbital energy differences are a combined consequence of the rather small charge difference and local geometry of the two zinc species.

The second point above is exemplified by the well-defined, single Zn2p core-level (1022.62 eV) and the

Zn3d valence band (11.47 eV) emissions referenced to the Si2p line at 103.38 eV in all materials studied. Moreover, data in Tables 4 and 5 show that most of the framework zinc substitutes for silicon (∼4 at. % of total T atoms in $NaZn_{synth}Y$ to 15% in $NaZn_{post}Y$) and a smaller part for aluminum (∼1% in $NaZn_{synth}Y$). This is a desirable result in that enhancement of ion-exchange capacity due to $Zn_{framework}$ on top of that due to $Al_{framework}$ is achieved.

The third point above demonstrates a practical value of the postsynthesis modification in that the total cation-exchange capacity due to combined $Zn_{framework}$ and $Al_{framework}$ in $NaZn_{post}Y$ is enhanced by a factor of 2 over that in NaY.

Acknowledgment. This research was carried out under the sponsorship of the Pennsylvania Infrastructure Technology Alliance and Air Products and Chemicals, Inc. APCI/PITA grant ADM-014. We gratefully acknowledge the allocation of time and services in the SCIENTA ESCA laboratory of Lehigh University. Professional assistance of Dr. Alfred Miller is greatly appreciated. A continued support of the Chemical Sciences U.S. DOE BES directorate to K.K. in the general area of surface science is also acknowledged.

CM0206690